

Communication

# NH<sub>3</sub> Sensor Based on ZIF-8/CNT Operating at Room Temperature with Immunity to Humidity

Wenjun Yan <sup>1,2,\*</sup>, Shiyu Zhou <sup>2</sup>, Min Ling <sup>2</sup>, XinSheng Peng <sup>2</sup> and Houpan Zhou <sup>1</sup><sup>1</sup> School of Automation, Hangzhou Dianzi University, Hangzhou 310018, China<sup>2</sup> Provincial Key Laboratory of Advanced Chemical Engineering Manufacture Technology, College of Chemical and Biological Engineering, Zhejiang University, Hangzhou 310027, China

\* Correspondence: yanwenjun@hdu.edu.cn

**Abstract:** Humidity effects on resistive gas sensors operating at room temperature remain a serious bottleneck. In this work, we introduce a resistive gas sensor based on a zeolitic imidazolate framework-8/carbon nanotube (ZIF-8/CNT) composite for the detection of ammonia gas at room temperature. The composite was prepared using a facile solution method. In this sensor, the basic mechanism was the charge transfer between ammonia molecules and CNTs; meanwhile, the ZIF-8 facilitated the adsorption of ammonia molecules as a preconcentrator, and prevented the adsorption of H<sub>2</sub>O molecules due to its hydrophobicity; CNTs were threaded through the ZIF-8 to form a great conductive network for charge transfer. The obtained sensor showed good ammonia sensing, especially at room temperature, with great selectivity and immunity to humidity under moderately humid conditions (45–70 % RH). However, the ammonia response was reduced at very high humidity (90% RH) due to the competitive adsorption of H<sub>2</sub>O molecules. This proved that the NH<sub>3</sub> sensor based on ZIF-8/CNT could be suitable for practical applications under moderately humid conditions.

**Keywords:** NH<sub>3</sub> sensor; ZIF-8/CNT; room temperature; immunity to humidity; hydrophobic



**Citation:** Yan, W.; Zhou, S.; Ling, M.; Peng, X.; Zhou, H. NH<sub>3</sub> Sensor Based on ZIF-8/CNT Operating at Room Temperature with Immunity to Humidity. *Inorganics* **2022**, *10*, 193. <https://doi.org/10.3390/inorganics10110193>

Academic Editor: Antonino Gulino

Received: 1 October 2022

Accepted: 27 October 2022

Published: 31 October 2022

**Publisher's Note:** MDPI stays neutral with regard to jurisdictional claims in published maps and institutional affiliations.



**Copyright:** © 2022 by the authors. Licensee MDPI, Basel, Switzerland. This article is an open access article distributed under the terms and conditions of the Creative Commons Attribution (CC BY) license (<https://creativecommons.org/licenses/by/4.0/>).

## 1. Introduction

Ammonia (NH<sub>3</sub>) is a highly toxic gas that is mostly released by industrial combustion and biological processes [1]. In direct contact, a high level of NH<sub>3</sub> irritates human skin, eyes, and respiratory tracts. A long-term (8 h) exposure level of 25 ppm and a short-term (15 min) exposure of 35 ppm have been set as the limits for ammonia [1]. Therefore, the design of a novel sensor allowing the sensitive and in-situ detection of ammonia is seriously essential. Ammonia sensors operating at low temperatures are especially more desirable because of the low power consumption, low cost, and good security.

Among various gas sensors, resistive sensors are most widely used due to their micro size and simple, portable setup. In the last decades, metal oxides, conductive polymer, carbon materials, transition-metal dichalcogenides, and even their hybrid-based nanostructures have been widely investigated for ammonia sensing [1–4]. Notably, humidity has a serious effect on the gas-sensing performances of room temperature (RT) sensors, which could result in unrepeatable and inaccurate measured responses. A hydrophobic surface is a common method to improve the immunity to the humidity of RT-gas-sensing materials. In existing reports, polypyrrole (PPy) and SnS<sub>2</sub> with ammonia-sensing behaviors were able to subdue the effect of humidity on ammonia sensing [5,6]. However, the simultaneous stability of an RT ammonia sensor remains a high challenge, due to the lack of thermal stability in PPy and SnS<sub>2</sub>.

A metal–organic framework (MOF) is constructed from metal ions or clusters coordinated to organic ligands, possessing a large surface area, tunable porosity, a hybrid organic–inorganic structure, and outstanding gas sorption properties [7–10]. Of particular note, ZIF-8, a kind of zeolitic imidazolate framework, has attracted much more attention

due to its high chemical and thermal stabilities and hydrophobicity [11–13]. As a result, it is also therefore very promising for gas sensing. However, ZIF-8-based hybrids, not solo ZIF-8, were usually taken as resistive gas-sensing materials due to their poor electrical conductivity. The ZIF-8 coating has been reported to improve the gas-sensing response as a preconcentrator [14], to improve the selectivity as a filter due to the tunable porosity [15,16], as well as to enhance immunity to humidity due to the hydrophobicity of ZIF-8 [17–19]. Carbon nanotubes (CNT) are well known for their outstanding electrical and mechanical properties, and thermal stability, and have therefore been widely studied within the last decades. CNT-based resistive sensors have been demonstrated to be sensitive to gas vapors at RT with low noise and high stability [20,21]. Unfortunately, disadvantages, such as low response value, long recovery time, and the strong influence of humidity limit the potential applications of CNT resistive sensors.

Inspired by previous works, we ideated that ZIF-8 stranding on CNT could obtain great  $\text{NH}_3$  sensing performances, which has not yet been reported to the best of our knowledge. Herein, the ZIF-8/CNT composite was prepared by a facile solution method. The  $\text{NH}_3$  sensing performances of the composite were investigated systematically, including under different humidity conditions. The ZIF-8/CNT showed a great  $\text{NH}_3$  response at room temperature with immunity to humidity. We also discuss the  $\text{NH}_3$  sensing mechanism of the ZIF-8/CNT composite.

## 2. Results and Discussion

### 2.1. Material Analysis

The SEM image in Figure 1a shows the morphology of the prepared ZIF-8/CNT. The rhombic dodecahedral morphology is ZIF-8, with a size of about 250 nm. The CNT is partially threaded through the ZIF-8, dedicated to the formation of an interconnected carbon nanotube network for the conductivity of the composite. The successful preparation of ZIF-8 is further confirmed by the XRD pattern (Figure 1b). The significant peaks at  $7.3^\circ$ ,  $10.4^\circ$ ,  $12.7^\circ$ ,  $14.7^\circ$ ,  $16.5^\circ$ , and  $18.1^\circ$  are attributed to (011), (002), (112), (022), (013), and (222) crystal planes of ZIF-8, respectively [22]. As shown in Figure S2, the CNT is multi-walled, and the measured spacing of the crystallographic plane is 0.34 nm from the high-resolution TEM image, corresponding to the (002) plane of CNT.

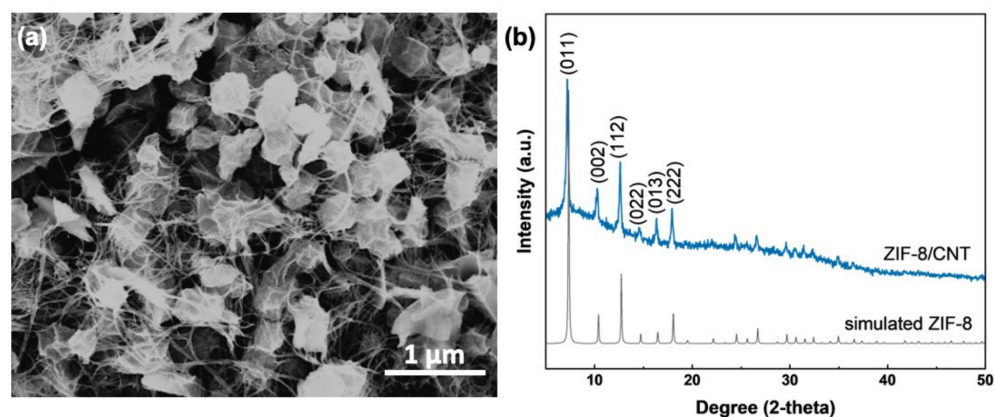


**Figure 1.** ZIF-8/CNT composite: (a) SEM image; (b) XRD pattern compared to that of simulated ZIF-8.

### 2.2. Sensor Fabrication and Gas-Sensing Test

The schematic of the bare sensor device with a pair of interdigital electrodes (IDEs) integrating with a microheater platform is shown in Figure 2a. The width of the Pt finger electrode was  $200\ \mu\text{m}$ , and the separation space between the coplanar platinum electrodes was  $100\ \mu\text{m}$ . For a completely resistive sensor device preparation,  $0.5\ \text{mg}$  as-prepared ZIF-8/CNT was dispersed in  $30\ \mu\text{L}$  of ethanol containing  $0.75\ \mu\text{L}$  of Nafion under ultrasonication for 10 min. One drop ( $\sim 1\ \mu\text{L}$ ) was then drop-casted onto the IDE area of a bare sensor chip. After that, the device was heated and maintained at  $80\ ^\circ\text{C}$  for 3 days to promote

sensing layer deposition and device aging to get reliable testing data. The inset of Figure 2b shows the optical image of the sensor device, as well as the sensing layer on IDEs. Ohmic contact was formed for the resistive sensing measurements between the sensing layer and IDEs, as demonstrated in Figure 2b.

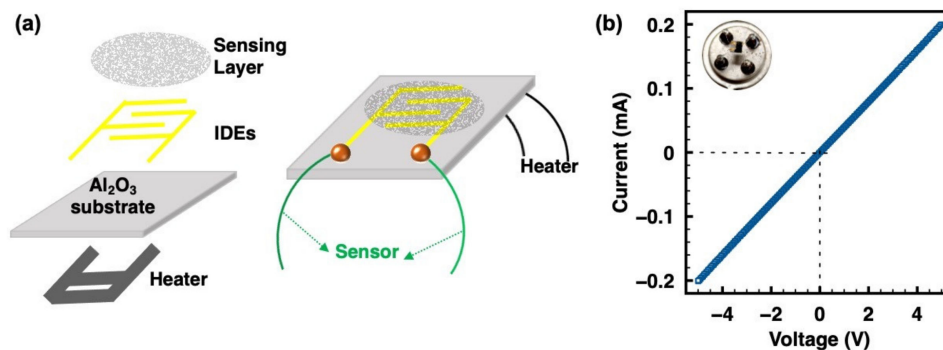


**Figure 2.** (a) Schematic diagram of the sensor device integrating with a microheater platform. (b) Linear I–V plot of the sensor device demonstrating Ohmic contact between the ZIF-8/CNT layer and IDEs; the inset is the optical image of the sensor device, showing the sensing layer on the IDEs.

The gas-sensing tests were performed using a self-made dynamic sensing measurement setup, which is described in detail in Figure S1 (Supplementary Materials). For all measurements, the ambient temperature was kept to around 25 °C and the sensor resistance was measured at 5 V. The response value was calculated as  $\Delta R/R_a$  in percentage, where  $\Delta R = R_g - R_a$ ,  $R_g$ , and  $R_a$  are the resistance of the sensor in a tested gas and air, respectively. The response/recovery time is defined as the time required for the sensor current change to reach 90% of the total resistance change.

### 2.3. Gas-Sensing Characteristics

The selectivity to several typical analytes (ammonia, ethanol, acetone, and formaldehyde) at 100 ppm, as displayed in Figure 3a, shows outstanding ammonia selectivity of the ZIF-8/CNT at RT. Figure 3b shows the response values of the ZIF-8/CNT to 100 ppm ammonia at different temperatures. The sample clearly exhibits the maximum response value ( $\sim 20$  at 100 ppm  $\text{NH}_3$ ) at RT of 25 °C. The response value decreases to about 12 at 100 ppm  $\text{NH}_3$  when the working temperature increases to the range of 50–110 °C. However, the higher operating temperature (50–110 °C) has no significant effect on the response value. For a surface-controlled gas sensor, the sensing response is the result of a dynamic equilibrium between adsorption and desorption [23]. At higher temperatures, the gas adsorption is higher and stronger, while the desorption is also improved. Therefore, the maximum response value of the ZIF-8/CNT to ammonia is obtained at RT. Figure 3c shows the continuous resistance variation of the ZIF-8/CNT to various ammonia concentrations (25–250 ppm) at RT. Upon exposure to ammonia, the composite resistance increases and then decreases back to the original value after the ammonia is turned off, indicating the complete response/recovery behavior and the p-type semiconductor behavior of the composite. The response/recovery time to ammonia in the range of 25–250 ppm is around 2/5 min. The response/recovery rate to ammonia gas needs to be improved in the next work. Figure 3d shows the positive linear relationship of response values to ammonia vs. concentration, suggesting the physisorption of ammonia molecules on the ZIF-8/CNT. The slope of the fitted curve (0.14388, as shown in Figure 3d) indicates the sensitivity of the device. Similar linear behavior has been reported for other MOF and CNT materials [24,25]. Additionally, the theoretical limit of detection (LOD) was calculated to be about 208 ppb when the signal-to-noise ratio is considered as 3 [26,27].

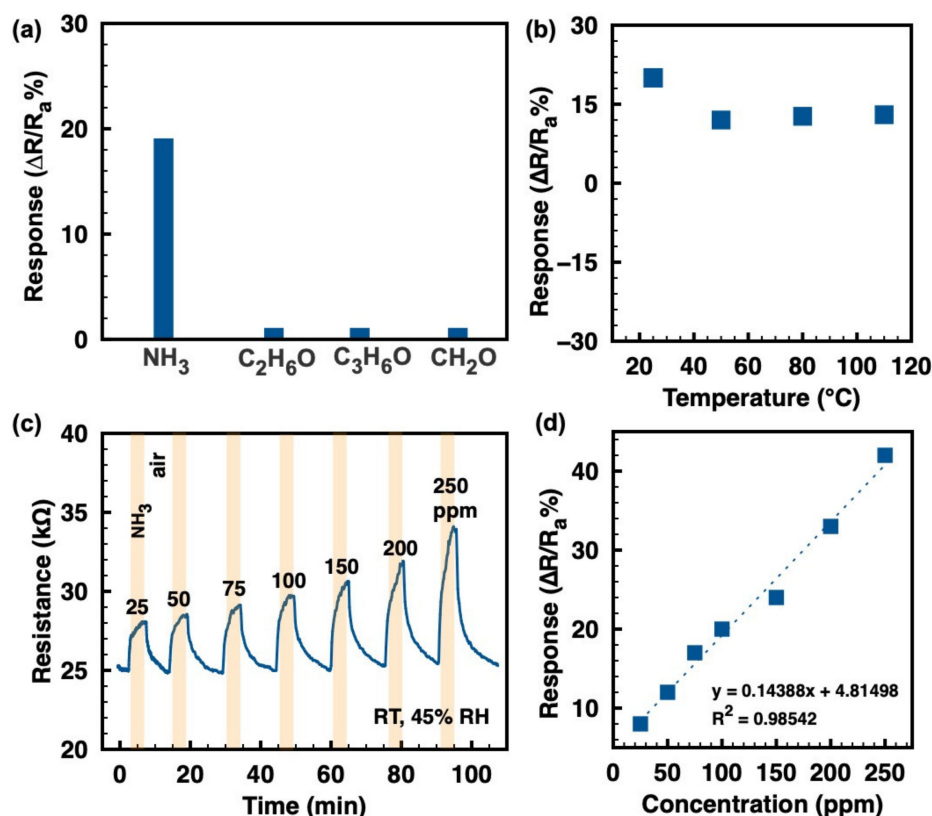


**Figure 3.** (a) Selectivity toward various gases (ammonia, ethanol, acetone, and formaldehyde) of 100 ppm at RT; (b) response values to 100 ppm ammonia at different working temperatures; (c) continuous resistance vs. time to ammonia at a variety of concentrations at RT; (d) the corresponding relationship of response values to ammonia and concentrations, with linear-fitting dashed lines.

As reported, CNT behaves as a p-type semiconductor, and the resistive response of CNT to gas molecules mainly depends on the change in electrical properties due to the charge transfer between the CNT and the gas molecules [25,28]. Since  $\text{NH}_3$  is a reducing agent,  $\text{NH}_3$  adsorption will inject electrons into the CNT and thus reduce the conducting hole number in the p-type CNT, thereby increasing the resistance. However, the interaction of CNT with gas molecules is very weak, leading to quite a poor response value [25]. In the present work, the ZIF-8 could allow the physisorption of more ammonia gas molecules as a preconcentrator, yielding more adsorption of  $\text{NH}_3$  on the CNT and a stronger interaction between them. Meanwhile, CNT threading through the ZIF-8 act as a transducer for resistive detection. Therefore, the enhanced ammonia sensing based on ZIF-8/CNT is proven.

Humidity is essential in real conditions and it must be taken into consideration, especially for room-temperature gas sensors. Figure 4a demonstrates that the ammonia responses of the ZIF-8/CNT show no obvious changes under moderately humid conditions (45–70%). However, at a higher humidity of 90%, the ammonia response is dramatically reduced. Figure 4b shows the contact angles of water droplets on the ZIF-8/CNT surface at 5 s and 2 min. The contact angle of  $71^\circ$  at 5 s and that of  $70^\circ$  at 2 min suggest a hydrophobic surface of ZIF-8/CNT, which contributes to the immunity of ammonia response to humidity in the range of 45–70%. However, at very high humidity levels (e.g., 90% RH), the ammonia response is dramatically reduced. This could be explained by the accumulation of excessive water molecules adsorbed on the material surface favoring the formation of  $\text{H}_3\text{O}^+$  ions, which hinders the adsorption of  $\text{NH}_3$  molecules [25].

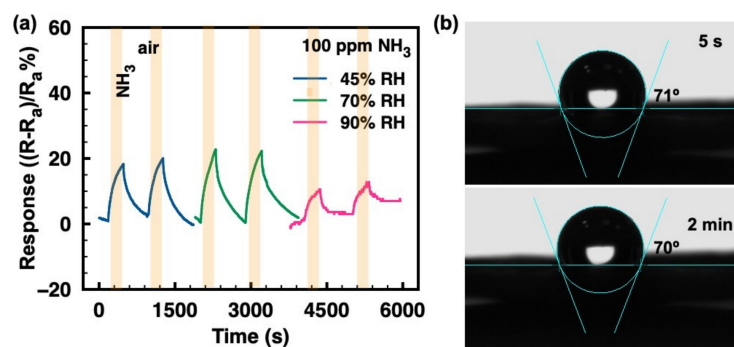


**Figure 4.** (a) Relative response vs. time to 100 ppm ammonia gas under different humidity atmospheres (45%, 70%, and 90%); (b) The contact angles of water droplets on the ZIF-8/CNT sample surface.

### 3. Materials and Methods

#### 3.1. ZIF-8/CNT Preparation

The ZIF-8/CNT was prepared according to the reference [29]. Briefly, 1.6 mM aminoethanol aqueous and 4 mM zinc nitrate aqueous were mixed under stirring, followed by aging for 30 min at room temperature, producing positively charged zinc hydroxide nanostrands (ZHN). Then, a certain amount of 0.5 mM carboxyl multi-walled carbon nanotubes (CNT, from XFNANO Materials Tech Co., Ltd., Nanjing, China) solution was added to the ZHN solution under strong stirring to become a homogeneous suspension. The volume ratio of ZHN to CNT is 30:1. The carboxyl CNT dispersed in water is negatively charged. Thus, zinc hydroxide nanostrands were strung by carbon nanotubes due to the electrostatic interaction. Next, the suspension was filtered to get ZHN/CNT powder. The ZIF-8/CNT was obtained by filtering after immersing the ZHN/CNT powder in 25 mM 2-methylimidazole (2-mIm) methanol–water (vol:vol = 2:3) solution for 24 h. The obtained ZIF-8/CNT was then washed with extra water and dried under vacuum at room temperature.

#### 3.2. Characterization

Scanning electron microscopy (SEM, ULTRA 55, Zeiss, Göttingen, Germany) was used to characterize the morphology of the prepared materials. Powder X-ray diffraction (XRD) analyses were performed on a Bruker D8 Advance diffractometer (Bruker, Berlin, Germany) with Cu K $\alpha$  radiation ( $\lambda \approx 1.54 \text{ \AA}$ ) to characterize the nanostructure of the samples.

### 4. Conclusions

In this study, a ZIF-8/CNT nanocomposite was facily prepared via a simple solution method. ZIF-8, with a rhombic dodecahedral morphology, facilitated the adsorption of ammonia molecules, while the CNT threading through the ZIF-8 formed an interconnected conductive network for the charge transfer between the ammonia molecules and the sensing material. Thus, the composite showed great ammonia-sensing performances at room temperatures, with great selectivity and immunity to humidity under moderately humid conditions (45–70 % RH), due to the hydrophobicity of ZIF-8. Unfortunately, under very high humid conditions (90% RH), the ammonia sensing of the ZIF-8/CNT was reduced due to the competitive adsorption of NH<sub>3</sub> and excessive H<sub>2</sub>O molecules.

**Supplementary Materials:** The following supporting information can be downloaded at: <https://www.mdpi.com/article/10.3390/inorganics10110193/s1>, Figure S1: Schematic view of gas-sensing setup. Inset shows the sensor device diagram; Figure S2: TEM images of ZIF-8/CNT.

**Author Contributions:** W.Y. and X.P. conceived the idea; S.Z. designed the experiments and carried out synthesis, and performed SEM and XRD characterizations; W.Y. designed and fabricated the device to perform gas-sensing measurements; W.Y. analyzed the data and wrote the manuscript; All authors analyzed and discussed the results. W.Y., M.L. and H.Z. directed the project. All authors have approved the final version of the manuscript.

**Funding:** This research was supported by the Zhejiang Science and Technology Foundation (LQ20F040006), and the Leading Innovative and Entrepreneur Team Introduction Program of Zhejiang (2019R01006).

**Institutional Review Board Statement:** Not applicable. This study doesn't involve humans or animals.

**Informed Consent Statement:** Not applicable.

**Data Availability Statement:** Not applicable.

**Acknowledgments:** W.Y. acknowledges the 2011 Zhejiang Regional Collaborative Innovation Center for Smart City. M.L. acknowledges the Leading Innovative and Entrepreneur Team Introduction Program of Zhejiang.

**Conflicts of Interest:** The authors declare no conflict of interest.

## References

1. Kwak, D.; Lei, Y.; Maric, R. Ammonia gas sensors: A comprehensive review. *Talanta* **2019**, *204*, 713–730. [[CrossRef](#)] [[PubMed](#)]
2. Vikrant, K.; Kumar, V.; Kim, K.-H. Graphene materials as a superior platform for advanced sensing strategies against gaseous ammonia. *J. Mater. Chem. A* **2018**, *6*, 22391–22410. [[CrossRef](#)]
3. Aarya, S.; Kumar, Y.; Chahota, R. Recent advances in materials, parameters, performance and technology in ammonia sensors: A review. *J. Inorg. Organomet. Polym. Mater.* **2020**, *30*, 269–290. [[CrossRef](#)]
4. Meng, Z.; Stolz, R.M.; Mendecki, L.; Mirica, K.A. Electrically-Transduced Chemical Sensors Based on Two Dimensional Nanomaterials. *Chem. Rev.* **2019**, *119*, 478–598. [[CrossRef](#)] [[PubMed](#)]
5. Huang, Y.; Jiao, W.; Chu, Z.; Wang, S.; Chen, L.; Nie, X.; Wang, R.; He, X. High sensitivity, humidity-independent, flexible NO<sub>2</sub> and NH<sub>3</sub> gas sensors based on SnS<sub>2</sub> hybrid functional graphene ink. *ACS Appl. Mater. Inter.* **2019**, *12*, 997–1004. [[CrossRef](#)]
6. Tang, X.; Raskin, J.-P.; Kryvutsa, N.; Hermans, S.; Slobodian, O.; Nazarov, A.N.; Debliquy, M. An ammonia sensor composed of polypyrrole synthesized on reduced graphene oxide by electropolymerization. *Sens. Actuators B Chem.* **2020**, *305*, 127423. [[CrossRef](#)]
7. Huang, X.; Huang, Z.; Zhang, L.; Liu, R.; Lv, Y. Highly efficient cataluminescence gas sensor for acetone vapor based on UIO-66 metal-organic frameworks as preconcentrator. *Sens. Actuators B Chem.* **2020**, *312*, 127952. [[CrossRef](#)]
8. Lu, W.G.; Wei, Z.W.; Gu, Z.Y.; Liu, T.F.; Park, J.; Park, J.; Tian, J.; Zhang, M.W.; Zhang, Q.; Gentle, T.; et al. Tuning the structure and function of metal-organic frameworks via linker design. *Chem. Soc. Rev.* **2014**, *43*, 5561–5593. [[CrossRef](#)]
9. Howarth, A.J.; Liu, Y.; Li, P.; Li, Z.; Wang, T.C.; Hupp, J.T.; Farha, O.K. Chemical, thermal and mechanical stabilities of metal-organic frameworks. *Nat. Rev. Mater.* **2016**, *1*, 1–15. [[CrossRef](#)]
10. Thunberg, J.; Zacharias, S.C.; Hasani, M.; Oyetunji, O.A.; Noa, F.M.A.; Westman, G.; Ohrstrom, L. Hybrid Metal-Organic Framework-Cellulose Materials Retaining High Porosity: ZIF-8@Cellulose Nanofibrils. *Inorganics* **2021**, *9*, 84. [[CrossRef](#)]
11. Cravillon, J.; Münzer, S.; Lohmeier, S.-J.; Feldhoff, A.; Huber, K.; Wiebcke, M. Rapid room-temperature synthesis and characterization of nanocrystals of a prototypical zeolitic imidazolate framework. *Chem. Mater.* **2009**, *21*, 1410–1412. [[CrossRef](#)]
12. Canivet, J.; Fateeva, A.; Guo, Y.M.; Coasne, B.; Farrusseng, D. Water adsorption in MOFs: Fundamentals and applications. *Chem. Soc. Rev.* **2014**, *43*, 5594–5617. [[CrossRef](#)]
13. Qin, Y.; Gui, H.; Bai, Y.; Xie, J. Moisture-Resistant Gas Sensor Derived from ZIF-8/Layered Double Hydroxide/Ti<sub>3</sub>C<sub>2</sub>T<sub>x</sub> Nanocomposites for Trace Isopropanol Detection. *ACS Appl. Nano Mater.* **2022**, *5*, 9799–9809. [[CrossRef](#)]
14. Ren, G.; Li, Z.; Yang, W.; Faheem, M.; Xing, J.; Zou, X.; Pan, Q.; Zhu, G.; Du, Y. ZnO@ZIF-8 core-shell microspheres for improved ethanol gas sensing. *Sens. Actuators B Chem.* **2019**, *284*, 421–427. [[CrossRef](#)]
15. Jafari, N.; Zeinali, S.; Shadmeh, J. Room temperature resistive gas sensor based on ZIF-8/MWCNT/AgNPs nanocomposite for VOCs detection. *J. Mater. Sci. Mater. Electron.* **2019**, *30*, 12339–12350. [[CrossRef](#)]
16. Khudiar, A.I.; Elttayef, A.K.; Khalaf, M.K.; Oufi, A.M. Fabrication of ZnO@ZIF-8 gas sensors for selective gas detection. *Mater. Res. Express* **2020**, *6*, 126450. [[CrossRef](#)]
17. Liu, Y.; Wang, R.; Zhang, T.; Liu, S.; Fei, T. Zeolitic imidazolate framework-8 (ZIF-8)-coated In<sub>2</sub>O<sub>3</sub> nanofibers as an efficient sensing material for ppb-level NO<sub>2</sub> detection. *J. Colloid Interface Sci.* **2019**, *541*, 249–257. [[CrossRef](#)]
18. Wang, Y.M.; Wang, X.C.; Qi, B.Y.; Cheng, J.P.; Wang, X.Y.; Shang, Y.Y.; Jia, J.F. Design of SnO<sub>2</sub>/ZnO@ZIF-8 Hydrophobic Nanofibers for Improved H<sub>2</sub>S Gas Sensing. *Chemistryselect* **2021**, *6*, 5488–5495. [[CrossRef](#)]
19. Nair, S.S.; Illyaskutty, N.; Tam, B.; Yazaydin, A.O.; Emmerich, K.; Steudel, A.; Hashem, T.; Schöttner, L.; Wöll, C.; Kohler, H. ZnO@ZIF-8: Gas sensitive core-shell hetero-structures show reduced cross-sensitivity to humidity. *Sens. Actuators B Chem.* **2020**, *304*, 127184. [[CrossRef](#)]
20. Li, J.; Lu, Y.; Ye, Q.; Cinke, M.; Han, J.; Meyyappan, M. Carbon nanotube sensors for gas and organic vapor detection. *Nano Lett.* **2003**, *3*, 929–933. [[CrossRef](#)]
21. Lupan, O.; Postica, V.; Mecklenburg, M.; Schulte, K.; Mishra, Y.K.; Fiedler, B.; Adelung, R. Low powered, tunable and ultra-light aerographite sensor for climate relevant gas monitoring. *J. Mater. Chem. A* **2016**, *4*, 16723–16730. [[CrossRef](#)]
22. Cheng, L.; Yan, P.; Yang, X.; Zou, H.; Yang, H.; Liang, H. High conductivity, percolation behavior and dielectric relaxation of hybrid ZIF-8/CNT composites. *J. Alloys Compd.* **2020**, *825*, 154132. [[CrossRef](#)]

23. Yoon, J.-W.; Kim, H.-J.; Kim, I.-D.; Lee, J.-H. Electronic sensitization of the response to C<sub>2</sub>H<sub>5</sub>OH of p-type NiO nanofibers by Fe doping. *Nanotechnology* **2013**, *24*, 444005. [[CrossRef](#)] [[PubMed](#)]
24. Jafari, N.; Zeinali, S. Highly rapid and sensitive formaldehyde detection at room temperature using a zif-8/mwcnt nanocomposite. *ACS Omega* **2020**, *5*, 4395–4402. [[CrossRef](#)]
25. Abdulla, S.; Mathew, T.L.; Pullithadathil, B. Highly sensitive, room temperature gas sensor based on polyaniline-multiwalled carbon nanotubes (PANI/MWCNTs) nanocomposite for trace-level ammonia detection. *Sens. Actuators B Chem.* **2015**, *221*, 1523–1534. [[CrossRef](#)]
26. Yan, W.J.; Chen, Y.L.; Zeng, X.M.; Wu, G.; Jiang, W.; Wei, D.; Ling, M.; Ng, K.W.; Qin, Y.X. Ultrasensitive ethanol sensor based on segregated ZnO-In<sub>2</sub>O<sub>3</sub> porous nanosheets. *Appl. Surf. Sci.* **2021**, *535*, 147697. [[CrossRef](#)]
27. Tang, H.; Li, Y.; Sokolovskij, R.; Sacco, L.; Zheng, H.; Ye, H.; Yu, H.; Fan, X.; Tian, H.; Ren, T.-L. Ultra-high sensitive NO<sub>2</sub> gas sensor based on tunable polarity transport in CVD-WS<sub>2</sub>/IGZO pN heterojunction. *ACS Appl. Mater. Inter.* **2019**, *11*, 40850–40859. [[CrossRef](#)]
28. Ong, K.G.; Zeng, K.; Grimes, C.A. A wireless, passive carbon nanotube-based gas sensor. *IEEE Sens. J.* **2002**, *2*, 82–88.
29. Liu, Y.Z.; Li, G.R.; Chen, Z.W.; Peng, X.S. CNT-threaded N-doped porous carbon film as binder-free electrode for high-capacity supercapacitor and Li-S battery. *J. Mater. Chem. A* **2017**, *5*, 9775–9784. [[CrossRef](#)]